Energy Dependence and Spectroscopy of the $^{16}O(p, d)^{15}O$ Reaction*

J. L. SNELGROVE† AND E. KASHY
Michigan State University, East Lansing, Michigan 48823

(Received 19 June 1969)

A systematic study of the extraction of spectroscopic factors for the (p, d) reaction on light nuclei and the difficulties encountered in obtaining reasonable distorted-wave Born approximation (DWBA) fits to the shapes of the angular distributions has been made. Deuteron spectra and angular distributions were measured for the $^{16}O(p, d)^{15}O$ reaction for 21.27-, 25.52-, 31.82-, 38.63-, and 45.34-MeV incident protons. The elastic scattering of protons from ^{16}O was measured over the same energy range and used to obtain proton optical-model parameters. Present results indicate that consistent spectroscopic information can be obtained from DWBA calculations when the deuterons in the exit channel have an energy greater than 20 MeV. Approximately 30% of the $1p_{3/2}$ strength appears to be missing from the 6.18-MeV, $\frac{3}{2}^-$ level of ^{15}O, and a large fraction of that strength appears in the 9.60- and 10.46-MeV levels. Small $2s$-$1d$ admixtures were observed in the ground state of ^{16}O, and excitation of a $\frac{7}{2}^+$ level is observed. This excitation is a possible candidate for a two-step excitation process.

I. INTRODUCTION

FOR a number of years the (p, d) reaction has proven to be a popular and valuable tool in nuclear spectroscopy. The selective way in which this reaction populates the levels of the residual nucleus provides information about these levels and about the ground state of the target nucleus, which can be compared to the predictions of various models which yield wave functions of nuclear states. The distorted-wave Born approximation (DWBA) theory of the direct reaction[1,2] has been widely used in the analysis of the (p, d) reaction to obtain spectroscopic information, which is usually given in terms of the spectroscopic factor. The meaningfulness of the spectroscopic factors, however, depends on the degree to which the DWBA calculation represents the actual reaction mechanism. In previous studies of (p, d) reactions on $1p$ shell[3–6] and $2s$-$1d$ shell[7,8] nuclei, difficulty was encountered in obtaining reasonable agreement between the experimental and DWBA angular distribution shapes when optical potentials which best described the elastic scattering were used in a standard DWBA calculation. The agreement was improved by the somewhat artificial means of adjusting optical potentials or using radial integration cutoffs, but in such cases one must be suspicious of the spectroscopic factors extracted. The present work was undertaken to study the use of the DWBA theory in the extraction of (p, d) spectroscopic factors for the light nuclei.

The nucleus ^{16}O was chosen for this study because its "closed" $1p$ shell nature and the numerous theoretical studies of its ground-state structure provided a basis for making predictions about the (p, d) spectroscopic factors to be expected, which could be used as a guide in evaluating the results of a given DWBA calculation. The strong dependence of the experimental peak of the $^{16}O(p, d)^{15}O$ $l_n=1$ angular distributions on the energy of the incident proton coupled with the availability of protons between 21 and 45 MeV made possible a test of energy dependence in the DWBA calculations. Similar studies have been made for the $^{40}Ca(d, p)^{41}Ca$ reaction[9] and for the $^{16}O(d, ^3He)^{15}N$ and $^{40}Ca(d, ^3He)^{39}K$ reactions.[10] Although the $^{16}O(p, d)^{15}O$ reaction has previously been studied with protons between 17 and 156 MeV,[7,11–16] it became clear as this study progressed that improved energy resolution made possible the extraction of additional spectroscopic information on the levels of ^{15}O, which is presented in some detail in this paper.

The elastic scattering of protons from ^{16}O was also studied at the various proton energies used in the (p, d) measurements in order to obtain optical-model parameters for use in the DWBA analysis. These data and parameters will be presented.

* Research supported by the National Science Foundation.
† Present address: Argonne National Laboratory, 9700 S. Cass Ave., Argonne, Ill. 60439.
[1] G. R. Satchler, Nucl. Phys. **55**, 1 (1964).
[2] R. H. Bassel, R. M. Drisko, and G. R. Satchler, Oak Ridge National Laboratory Report No. ORNL-3240, 1962 (unpublished); R. H. Bassel, R. M. Drisko, and G. R. Satchler, Oak Ridge National Laboratory Memorandum to the Users of the Code JULIE, 1966 (unpublished).
[3] L. A. Kull, Ph.D. thesis, Michigan State University, 1967 (unpublished).
[4] L. A. Kull, Phys. Rev. **163**, 1066 (1967).
[5] L. A. Kull and E. Kashy, Phys Rev. **167**, 963 (1968).
[6] R. L. Kozub, L. A. Kull, and E. Kashy, Nucl. Phys. **A99**, 540 (1967).
[7] R. L. Kozub, Ph.D. thesis, Michigan State University, 1967 (unpublished).
[8] R. L. Kozub, Phys. Rev. **172**, 1078 (1968).
[9] L. L. Lee, Jr., J. P. Schiffer, B. Zeidman, G. R. Satchler, R. M. Drisko, and R. H. Bassel, Phys. Rev. **136**, B971 (1964).
[10] J. C. Hiebert, E. Newman, and R. H. Bassel, Phys. Rev. **154**, 898 (1967).
[11] N. W. Chant, P. S. Fisher, and D. K. Scott, Nucl. Phys. **A99**, 669 (1967).
[12] G. G. Shute and R. E. Brown, University of Minnesota Linear Accelerator Laboratory Annual Progress Report No. 55, 1967 (unpublished).
[13] J. C. Legg, Phys. Rev. **129**, 272 (1963).
[14] J. K. P. Lee, S. K. Mark, P. M. Portner, and R. B. Moore, Nucl. Phys. **A106**, 357 (1967).
[15] D. Bachelier, M. Bernas, I. Brissand, C. Detraz, N. K. Ganguly, and P. Radvangi, Compt. Rend. **2**, 429 (1964).
[16] I. S. Towner, Nucl. Phys. (to be published).

II. EXPERIMENTAL APPARATUS AND METHODS

The proton beam of the Michigan State University sector-focused cyclotron was magnetically analyzed and focused on target at the center of a 36-in. scattering chamber. The energy, resolution, and divergence of the beam were determined from settings of the analysis system, which has been described elsewhere.[17]

The target was natural oxygen gas (99.76% ^{16}O) at approximately 30-cm Hg pressure contained in either a 3- or 5-in. cell with a 0.0005-in. Kapton[18] window. The detector used in the (p, p) experiments was a 0.25-in.-square, 0.50-in.-thick CsI(Tl) crystal mounted on the face of a photomultiplier tube. Most of the (p, d) data were obtained with commercial silicon detectors in a standard ΔE-E arrangement, using a Goulding system for particle identification, with a typical energy resolution of 110 keV for 45-MeV incident protons, a large fraction of which was attributable to kinematic broadening. In one experiment, particle identification was accomplished using a single counter with time-of-flight techniques, with a resolution of 60 keV for 32-MeV incident protons.

Angular distributions were taken in 5° steps from $\theta_{lab}=\sim 10°$ to 70° and in 7.5° steps from $\theta_{lab}=70°$ to 160°. Additional points were often taken between 10° and 20° to determine better the first peak of the angular distribution. Measurements were made on both sides of the beam to determine any zero correction to the digital readout of the scattering angle.

The energy spectra were analyzed on the Laboratory's Scientific Data Systems Sigma 7 computer to determine the mean energy and yield of each state seen. The energies were corrected for the energy lost in the gas and cell walls by the incident and scattered particles. The yields were corrected for background in all experiments, and in the (p, p) experiments corrections were made for analyzer dead time (typically $\leq 2\%$) and for counting losses due to reactions in the CsI(Tl) crystal ($\leq 2\%$). Differential cross sections were calculated using the geometrical corrections for gas-cell geometry given by Silverstein.[19] The total measurement uncertainty in the differential cross sections is estimated to be 3.6% at $\theta_{lab}\simeq 30°$. The error bars shown on all data represent the total uncertainty, i.e., the measurement uncertainty and the statistical uncertainty added in quadrature. A more detailed description of the experimental methods and the treatment of errors is contained in Ref. 20.

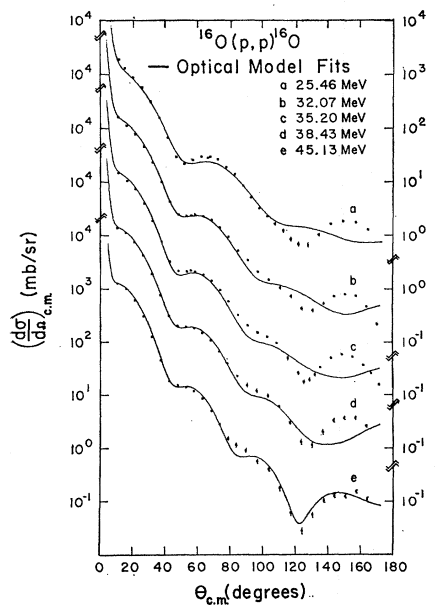

FIG. 1. Optical-model fits to the $^{16}O(p, p)^{16}O$ angular distributions using energy-dependent sets of parameters.

III. ELASTIC SCATTERING DATA AND OPTICAL-MODEL PARAMETERS

A. Proton Scattering

Differential cross sections for the elastic scattering of protons by ^{16}O were measured at incident energies of 25.46, 32.07, 35.10, 38.43, and 45.13 MeV over an angular range of 10° to 170° in the c.m. frame. After completing each angular distribution, measurement of the differential cross section at the position of the second maximum (50°–60°) over an energy range of ±300 keV around the bombarding energy showed that no sharp resonances existed. As a check on the efficiency of the counter system, differential cross sections for the elastic scattering of protons by protons were measured at several angles between 15° and 22° in the laboratory frame. These were compared to those measured by Johnston and Swenson[21] and were found to agree within the experimental errors. The $^{16}O(p, p)$ angular distributions are shown in Fig. 1. These data are in quantitative agreement with those of Cameron *et al.*[22,23] whose extensive study covered the energy range 23.4–46.1 MeV. They found that the behavior of the cross sections below 30 MeV indicated the existence of broad resonances in the p-^{16}O system. These resonances were too broad to have been detected during the search for sharp resonances within 300 keV of the original proton energy.

In the optical model of elastic scattering, it is assumed that the interaction of the two nuclei involved can be represented by scattering from a one-body complex

[17] G. H. Mackenzie, E. Kashy, M. M. Gordon, and H. G. Blosser, IEEE Trans. Nucl. Sci. **NS-14**, 450 (1967).
[18] E. I. Dupont de Nemours, Wilmington, Del.
[19] E. A. Silverstein, Nucl. Instr. Methods **4**, 53 (1959).
[20] J. L. Snelgrove, Ph.D. thesis, Michigan State University, 1968 (unpublished).
[21] L. H. Johnston and D. A. Swenson, Phys. Rev. **111**, 212 (1958).
[22] J. M. Cameron, University of California at Los Angeles Technical Report No. P-80, 1967 (unpublished).
[23] J. M. Cameron, J. R. Richardson, W. T. H. van Oers, and J. W. Verba, Phys. Rev. **167**, 908 (1968).

TABLE I. Optical-model parameters describing proton elastic scattering from ^{16}O.

E_p(lab) (MeV)	V (MeV)	W_S (MeV)	W_D (MeV)	r_I (E)	a_I (F)	σ_R(expt)[a] (mb)	σ_R(theoret.) (mb)	χ^2/N
25.46	48.4	0.0	6.80	1.19	0.550	507	535	36.7
32.07	45.5	0.0	5.31	1.44	0.490	473	487	32.3
35.20	45.0	0.91	5.70	1.45	0.450	458	498	45.3
38.43	44.4	2.00	4.89	1.40	0.430	441	446	16.5
45.13	42.7	3.11	5.65	1.28	0.415	407	407	4.9

$r_{so}=r_R=1.12$ F, $a_{so}=a_R=0.69$ F, $r_c=1.15$ F, $V_{so}=7.0$ MeV

[a] Based on data found in Ref. 22.

potential having the form

$$V_{opt}(r)=V_c(r)-Vf(x)-i[W_S-4W_D(d/dx')]f(x')+V_{so}[(\hbar)^2/(m_\pi c)^2]r^{-1}[df(x)/dr](\boldsymbol{l}\cdot\boldsymbol{\sigma}),$$

where

$$V_c(r)=ZZ'e^2/r, \quad r\geq R_c$$
$$=ZZ'e^2[3-(r^2/R_c^2)]/2R_c, \quad r\leq R_c$$
$$R_c=r_cA^{1/3},$$

and

$$f(x)=(e^x+1)^{-1},$$

with

$$x=(r-r_RA^{1/3})/a_R,$$
$$x'=(r-r_IA^{1/3})/a_I.$$

V_c is the potential felt by a point charge Ze interacting with a uniformly charged sphere of radius R_c and charge $Z'e$.

Optical-model analyses were performed with the Perey search code GIBELUMP,[24] with the spin-orbit radius and diffuseness set equal to the corresponding real-well parameters. The initial calculations were constrained to give a single set of parameters which gave the best over-all fit to the five experimental angular distributions. However, owing to nonlocality effects not included in the optical potential, one expects the parameters to exhibit some energy dependence, so subsequent searches allowed the parameters to vary with the incident proton energy. The real radius and diffuseness tended not to vary and so were fixed. The angular distribution fits were found to be very insensitive to changes in V_{so}.

A value of 7.0 MeV for V_{so} was chosen on the basis of parameters found by Cameron[22] during preliminary analyses of elastic scattering[23] and polarization data.[25] Cameron[22] had also measured reaction cross-section data at incident proton energies appropriate to his work. Since these varied smoothly with energy, values of the reaction cross section σ_R for the incident proton energies of the present work were extracted by graphical interpolation. These were used as a guide in choosing between sets of optical parameters which gave essentially identical values of χ^2/N.

The final set of parameters is shown in Table I, and the corresponding fits are shown in Fig. 1. It was found that inclusion of a volume imaginary potential was necessary above 32.07 MeV, with its strength increasing with energy. This is probably due to the deeper penetration of the more highly energetic protons. The forward angle fits are improved, although the improvement is slight for the 25.46-MeV data. The back angle fits are very poor for all but the 45.13-MeV data. This behavior is consistent with that found by van Oers and Cameron[26] over the energy range of 23–53 MeV, by Barrett *et al.*[27] at 30.3 MeV, by Kim *et al.*[28] at 31.0 MeV, and by Fannon *et al.*[29] at 49.48 MeV. It has been found in other work[30] that the use of a spin-orbit radius parameter 10 to 15% smaller than the real radius parameter was helpful in obtaining fits to the back angle data. This was tried with no significant improvement. Thus, it appears that the optical model gives a poor description of proton elastic scattering from ^{16}O below 30 MeV where resonances occur, that between 30 and 40 MeV the description is good forward of 100° and that the

TABLE II. Deuteron optical parameters used in the DWBA analysis of the $^{16}O(p,d)^{15}O$ reaction.

E_d (MeV)	V (MeV)	r_R (F)	a_R (F)	W_D (MeV)	r_I (F)	a_I (F)
33.2	92.8	1.03	0.80	8.84	1.41	0.70
26.2	98.0	1.00	0.80	7.95	1.45	0.70
19.0	104.0	0.98	0.80	7.05	1.50	0.70
10.4	114.0	0.95	0.80	6.00	1.57	0.70
4.5	130.0	0.90	0.80	5.00	1.68	0.70

$r_{so}=r_R$, $a_{so}=a_R$, $V_{so}=7.57$ MeV, $r_{oc}=1.30$ F.

[24] Unpublished FORTRAN-IV computer code written by F. G. Perey and modified by R. M. Haybron at Oak Ridge National Laboratory.

[25] H. B. Eldridge, S. N. Bunker, J. M. Cameron. J. R. Richardson, and W. T. H. van Oers, Phys. Rev. **167**, 915 (1968).

[26] W. T. H. van Oers and J. M. Cameron, Bull. Am. Phys. Soc. **13**, 883 (1968).

[27] R. C. Barrett, A. D. Hill, and P. E. Hodgson, Nucl. Phys. **62**, 133 (1965).

[28] C. C. Kim. S. M. Bunch, D. W. Devins, and H. H. Forster, Nucl. Phys. **58**, 32 (1964).

[29] J. A. Fannon, E. J. Burge, D. A. Smith, and N. K. Ganguly, Nucl. Phys. **A97**, 263 (1967).

[30] M. P. Fricke, E. E. Gross, B. J. Morton, and A. Zucker, Phys. Rev. **156**, 1207 (1967).

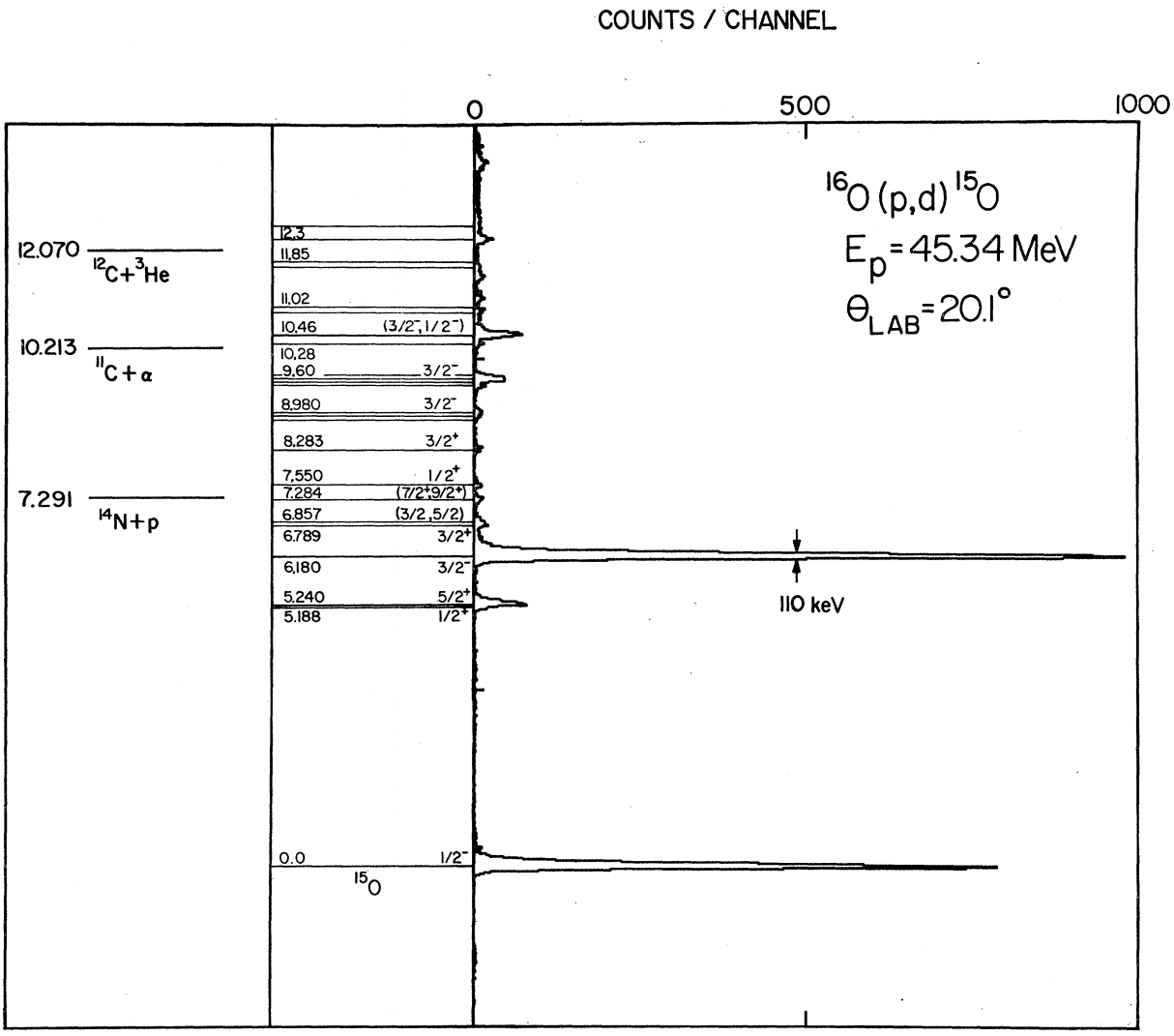

FIG. 2. Energy-level diagram of ^{15}O displayed beside a deuteron energy spectrum from the $^{16}O(p, d)^{15}O$ reaction for $E_p = 45.34$ MeV and $\theta_{lab} = 20.1°$.

optical model describes the scattering very well for incident protons above 40 MeV.

B. Deuteron Scattering

Since it is impossible to measure the elastic scattering of deuterons by the unstable nucleus ^{15}O, data for deuteron scattering by ^{16}O was used. Sets of optical-model parameters have been found for deuteron elastic scattering by ^{16}O for incident deuteron energies between 11.8 and 52 MeV.[31–37] Many studies have been done with lower energy deuterons, but the applicability of the optical model is questionable in these cases. The parameters used here are based on the 11.8-MeV parameters of Hodgson,[34] the 34.4-MeV parameters of Newman *et al.*,[36] and the 52-MeV parameters of Duelli *et al.*[37] Each of these studies used a derivative surface absorption and included spin-orbit effects. The various parameters were plotted with respect to deuteron energy and smooth curves weighted toward the 34.4-MeV parameters and away from the 16.8-MeV parameters were used to determine the parameters to be used in the (p, d) analyses. They are listed in Table II.

IV. EXPERIMENTAL RESULTS

In this section spectra and angular distributions are presented for the $^{16}O(p, d)^{15}O$ reaction. Some of the conclusions reached about possible spin and parity assignments are based upon the DWBA calculations discussed in the next section.

[31] W. Fitz, R. Jahr, and R. Santo, Nucl. Phys. **A101**, 449 (1967).
[32] Dai-Ca Nguyen, J. Phys. Soc. Japan **21**, 2462 (1966).
[33] A. A. Cowley, G. Heymann, R. L. Keizer, and M. J. Scott, Nucl, Phys. **86**, 363 (1966).
[34] P. E. Hodgson, Advan. Phys. **15**, 329 (1966), quoted in Ref. 11.
[35] J. Testoni, S. Mayo, and P. E. Hodgson, Nucl. Phys. **50**, 479 (1964).
[36] E. Newman, L. C. Becker, B. M. Preedom, and J. C. Hiebert, Nucl. Phys. **A100**, 225 (1967).
[37] B. Duelli, F. Hintenberger, G. Mairle, U. Schmidt-Rohr, P. Turek, and G. Wagner, Phys. Letters **23**, 485 (1966).

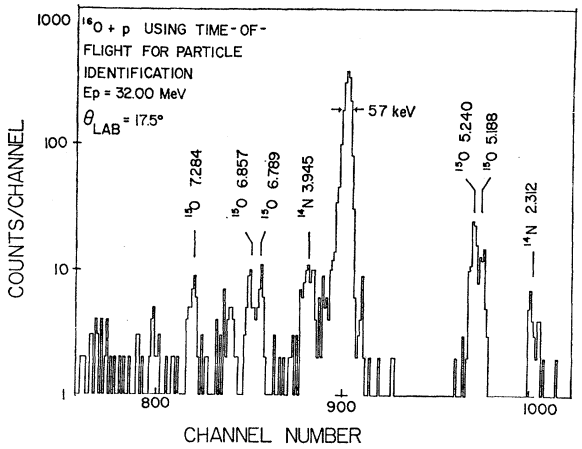

FIG. 3. Energy spectrum of reaction products at $\theta_{lab}=17.5°$ for 32.00-MeV protons incident on ^{16}O, obtained by use of time-of-flight techniques for particle identification.

A. Simple Model Predictions

Considered as a direct reaction, the (p, d) reaction involves the removal of a single neutron from the target nucleus, which is assumed to be in its ground state. The single-particle energies are given by Jolly[38] as 0.0, 27.0, 33.0, 44.0, and 45.0 MeV for the $1s_{1/2}$, $1p_{3/2}$, $1p_{1/2}$, $1d_{5/2}$, and $2s_{1/2}$ particles, respectively. Thus, for the low-lying levels one would expect either a $1p_{1/2}$ or a $1p_{3/2}$ neutron to be picked up; the pickup of a $1s_{1/2}$ neutron would be very unlikely owing to its strong binding. On this basis, one would expect the deuteron energy spectra to contain one $\frac{1}{2}^-$ peak, one $\frac{3}{2}^-$ peak, and no others.

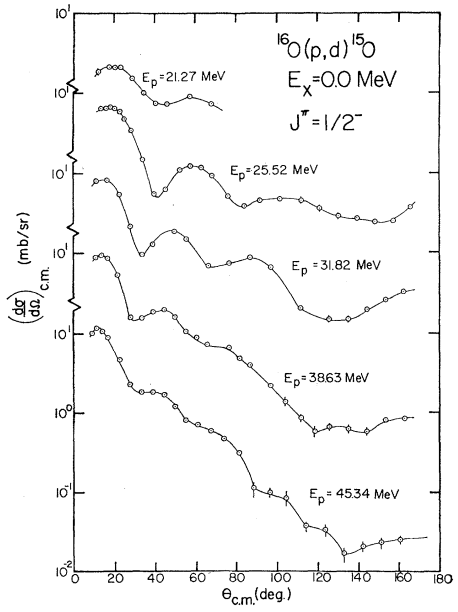

FIG. 4. Experimental deuteron angular distributions for the 0.0-MeV, $\frac{1}{2}^-$ level of ^{15}O from the ^{16}O$(p, d)^{15}$O reaction for incident proton energies between 21.27 and 45.34 MeV.

[38] H. P. Jolly, Phys. Letters **5**, 289 (1963).

It is known, however, that the simple model is much too naive, even for the case of a "closed-shell" nucleus such as ^{16}O. One might consider the effects of low-lying deformed states in the closed-shell nucleus[39–42] when using that nucleus as a core. Brown and Shukla[43] have performed such calculations for ^{15}O and ^{15}N. They predict, in addition to the strong 0.0-MeV, $\frac{1}{2}^-$ and 6.18-MeV, $\frac{3}{2}^-$ levels, the existence of a $\frac{3}{2}^-$ level between 10.0 and 11.0 MeV of excitation and a $\frac{1}{2}^-$ level approximately 1.0 MeV lower. Bertsch[44] has predicted that core polarization could result in many highly fragmented states with excitation energies of approximately 20 MeV. Hence, core polarization can result in the sharing

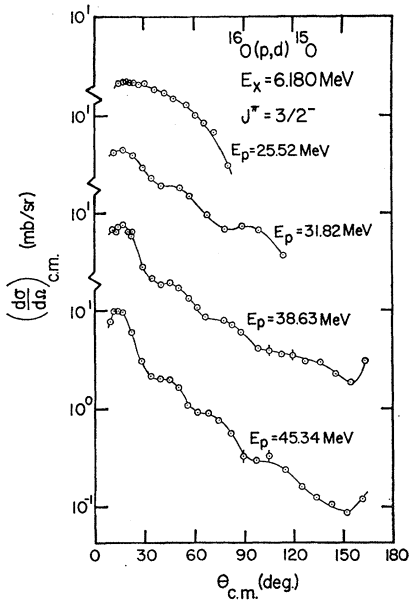

FIG. 5. Experimental deuteron angular distributions for the 6.180-MeV, $\frac{3}{2}^-$ level of ^{15}O from the ^{16}O$(p, d)^{15}$O reaction for incident proton energies between 25.52 and 45.34 MeV.

of the $1p_{1/2}$ and $1p_{3/2}$ strengths among several states. One would also expect the ^{16}O ground state to be more complex. Calculations have been performed[41] in which two-particle–two-hole and four-particle–four-hole admixtures have been considered. If such admixtures existed, one would expect to pickup some $1d_{5/2}$ and $2s_{1/2}$ neutrons, leading to positive parity levels in ^{15}O.

B. Energy Spectra

Figure 2 shows an energy-level diagram (including all known levels below 11 MeV) of the ^{15}O nucleus beside which has been placed a deuteron spectrum taken at a laboratory angle of 20.1° with 45.34-MeV incident

[39] H. Morinaga, Phys. Rev. **101**, 254 (1956).
[40] T. Engeland, Nucl. Phys. **72**, 68 (1965).
[41] G. E. Brown and A. M. Green, Nucl. Phys. **75**, 401 (1966).
[42] G. E. Brown and A. M. Green, Nucl. Phys. **85**, 87 (1966).
[43] G. E. Brown and A. P. Shukla, Princeton University Report No. PUC-937-268, 1967 (unpublished).
[44] G. F. Bertsch (private communication).

protons. All energies, spins, and parities for the levels below 9 MeV were taken from the γ-ray work of Warburton *et al.*,[45] those of the levels between 9 and 10 MeV from the work of Lambert and Durand,[46] and those of levels above 10 MeV from Lauritsen and Ajzenberg-Selove.[47] One immediately notices in Fig. 2 the presence of the two very strong peaks corresponding to $1p_{1/2}$ and $1p_{3/2}$ neutron pickup with all other states being much more weakly excited. Figure 3 shows a spectrum obtained using the time-of-flight system for mass identification in which the closely spaced levels near 5.2 and 6.8 MeV are partially resolved. The peaks corresponding to ^{14}N levels are due to ^{3}He particles from the $^{16}O(p, ^{3}He)^{14}N$ reaction which reached the detector within the accepted time window. Other spectra showing comparable resolution were obtained with this method at laboratory angles between 12.4° and 30°.

C. Negative-Parity Levels

Below an excitation energy of 16.5 MeV, the existence of one $\frac{1}{2}^-$ and three $\frac{3}{2}^-$ levels have been confirmed.[45–47] Angular distributions measured for the 0.0-MeV, $\frac{1}{2}^-$ and 6.180-MeV, $\frac{3}{2}^-$ levels predicted by the simplest shell model are shown in Figs. 4 and 5. A first maximum between 10° and 20° in the c.m. frame is characteristic of $l_n=1$ pickup, with the angle at which the first maximum occurs decreasing as the incident proton energy increases. J dependence in this reaction exhibits itself in the generally steeper slope and more pronounced oscillation of the $J^\pi=\frac{1}{2}^-$ angular distributions.

The magnitude of the differential cross section at the first $l_n=1$ maximum, which is used in the extraction of spectroscopic factors, is shown as a function of the incident proton energy in Fig. 6. Included in this figure are points from other studies of the $^{16}O(p, d)^{15}O$ reaction between 18.5 and 100 MeV.[7,11–14] The dashed curves are drawn to accentuate the general trend of the data and indicate that the $\frac{3}{2}^-$ peak cross section becomes larger than the $\frac{1}{2}^-$ peak cross section at some point between 45 and 100 MeV. Data by Bachelier *et al.*[15] at 156 MeV, which are not shown, indicate that the peak cross sections drop to approximately 5.2 mb/sr and approximately 8.3 mb/sr for the 0.0- and 6.180-MeV levels, respectively.

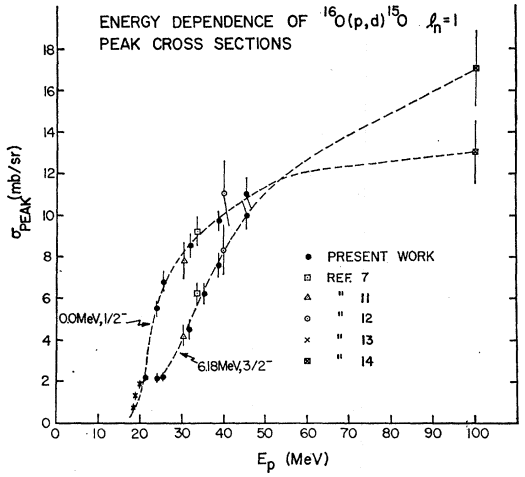

FIG. 6. Dependence of the $l_n=1$ peak cross section of the 0.0-MeV, $\frac{1}{2}^-$ and 6.180-MeV, $\frac{3}{2}^-$ levels of ^{15}O from the $^{16}O(p, d)^{15}O$ reaction on the incident proton energy.

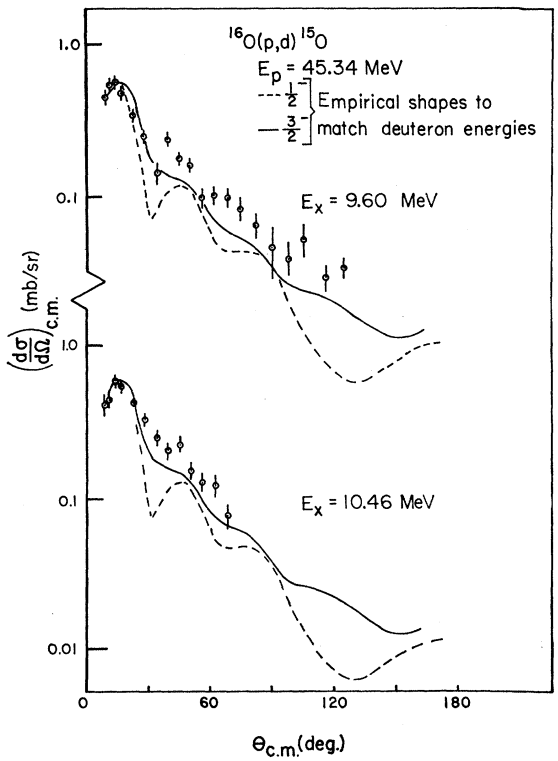

FIG. 7. Deuteron angular distributions for the 9.60- and 10.46-MeV levels of ^{15}O from the $^{16}O(p, d)^{15}O$ reaction for $E_p=45.34$ MeV.

Figure 2 shows the presence of two relatively strong deuteron groups corresponding to levels of higher excitation energy. The first group corresponds to the levels at 9.49, 9.53, 9.60, and 9.66 MeV, which have $J^\pi=\frac{5}{2}^-$, $\frac{1}{2}^+$, $\frac{3}{2}^-$, and $(\frac{7}{2}, \frac{9}{2})^-$, respectively.[46] Careful examination of the energy spectra showed that all four levels were excited, but that approximately 70% of the yield was due to excitation of the 9.60-MeV, $\frac{3}{2}^-$ level. The other deuteron group comes from the excitation of the 10.46-MeV level, which was resolved from the 10.28-MeV level. Angular distributions for these levels are shown in Fig. 7. The angular distribution labeled 9.60 contains contributions from the other three close-lying levels. The curves represent empirical $l_n=1$ shapes corresponding to the Q values of the reactions leading to these states, obtained by graphical inter-

[45] E. K. Warburton, J. W. Olness, and D. E. Alburger, Phys. Rev. 140, B1202 (1965).
[46] M. Lambert and M. Durand, Phys. Letters 24B, 287 (1967).
[47] T. Lauritzen and F. Ajzenberg-Selove, in *Nuclear Data Sheets*, compiled by K. Way *et al.* (Printing and Publishing Office, National Academy of Sciences—National Research Council, Washington 25, D. C., 1962).

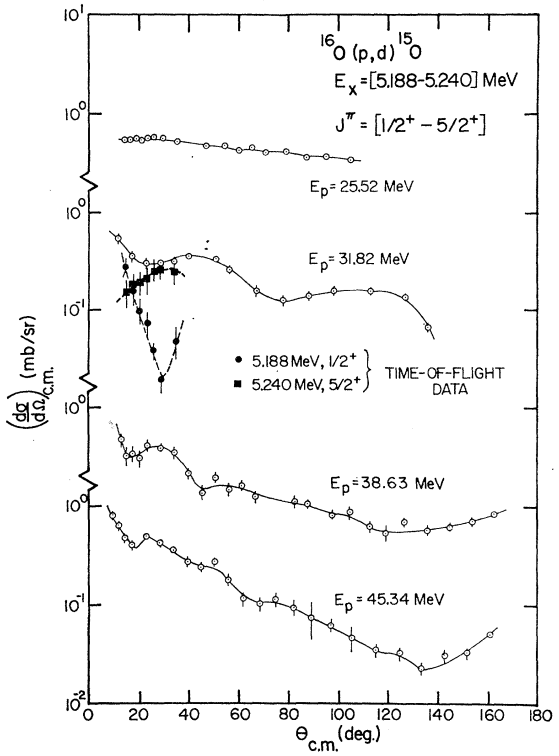

FIG. 8. Deuteron angular distributions for the 5.188–5.240 MeV doublet of ^{15}O from the ^{16}O$(p, d)^{15}$O reaction for incident proton energies between 25.52 and 45.34 MeV.

polation between the shapes of the 0.0 and 6.18 MeV angular distributions for 45.34- and 38.62-MeV incident protons. Both levels are seen to be $l_n=1$ in character, the assignment of $\frac{3}{2}^-$ to the 10.46-MeV level being preferred on the basis of shape. The angular distribution for the 9.60-MeV level does not disagree with the previous $\frac{3}{2}^-$ assignment for that level. Estimates of the $1p_{3/2}$ hole strength in these levels will be given in Sec. V, where spectroscopic factors will be discussed.

D. Positive-Parity Levels

As was noted previously, the only way in which a positive-parity level can be reached in ^{15}O by the direct pickup of a neutron from ^{16}O is for the ^{16}O ground state to contain an admixture of even-l neutrons. The most likely admixtures being $1d_{5/2}$ and $2s_{1/2}$ neutrons, one would look for $\frac{5}{2}^+$ and $\frac{1}{2}^+$ levels. The levels at 5.188, 7.550, 8.735, and 9.53 have previously been shown to be $\frac{1}{2}^+$. The level at 5.240 MeV has an assignment of $\frac{5}{2}^+$, and the $(\frac{3}{2}, \frac{5}{2})$ level at 6.857 MeV appears to be the mirror level of the 7.15 MeV, $\frac{5}{2}^+$ level in ^{15}N.

Examination of Figs. 2 and 3 shows that the 5.188–5.240-MeV doublet has considerable strength. Angular distributions for the unresolved doublet are shown in Fig. 8. The time-of-flight data taken with 32.0-MeV incident protons had sufficient resolution to allow a Gaussian peak shape analysis to be performed to separate the states. Using a nonlinear least-squares method, a skewed Gaussian was fitted to the single 6.18-MeV level to determine a peak shape. Then the areas and centroids of two Gaussians having this shape were adjusted, keeping a fixed separation corresponding to the known separation of the levels, until the fit to the 5.188–5.240-MeV group was judged best. The ratios of the areas were applied to the 31.82-MeV data to obtain partial angular distributions, also shown in Fig. 8. The large errors (approximately 30%) are due to the poor statistics of the data and the uncertainty in the ratios of the areas. The shape of the 5.188 MeV angular distribution is characteristic of $l_n=0$ pickup, whereas the occurrence of the first maximum near 30° for the 5.240-MeV angular distribution indicates an $l_n\geq 2$, consistent with the $\frac{5}{2}^+$ assignment. This disagrees with ^{16}O$(d, t)^{15}$O data quoted in Ref. 48, which showed no direct reaction pattern for the $\frac{1}{2}^+$ member of the doublet.

Excitations of the other $\frac{1}{2}^+$ and $\frac{5}{2}^+$ levels are very weak, with the exception of the 7.550 MeV, $\frac{1}{2}^+$ level, which does not exhibit the characteristics of $l_n=0$ pickup (Fig. 10). Wong[48] in a study of centroids and sums of direct reaction strengths with ^{16}O as a target, has found that central-force (e.g., Rosenfeld and Soper) calculations imply that most of the $1d_{5/2}$ strength is in the 5.24-MeV level, whereas calculations using realistic forces (e.g., Brueckner-Gamel-Thaler, Hamada-Johnston) imply that the dominant part of the $1d_{5/2}$ strength will be in a higher $\frac{5}{2}^+$ state. Thus, the present data tend to support the use of central forces.

Weak excitation of the $\frac{3}{2}^+$ levels at 6.789 and 8.283 MeV has been found, which could be due to the pickup of a $1d_{3/2}$ neutron. The shapes of the angular distributions (Fig. 10) are not inconsistent with such a pickup. An interesting angular distribution was measured for the level at 7.284 MeV, which had been assigned a spin of $\leq\frac{9}{2}$ and appears to be the mirror level of the 7.56-MeV,

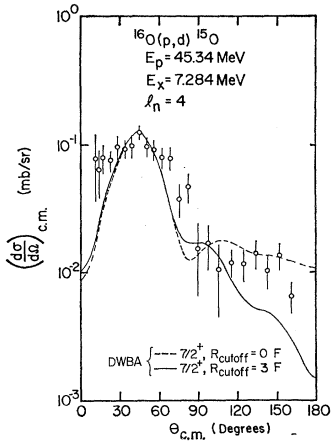

FIG. 9. Deuteron angular distribution and DWBA fit for the 7.284-MeV, $(\frac{7}{2}^+)$ level of ^{15}O from the ^{16}O$(p, d)^{15}$O reaction for E_p=45.34 MeV.

[48] S. S. M. Wong, Nucl. Phys. **A120**, 625 (1968).

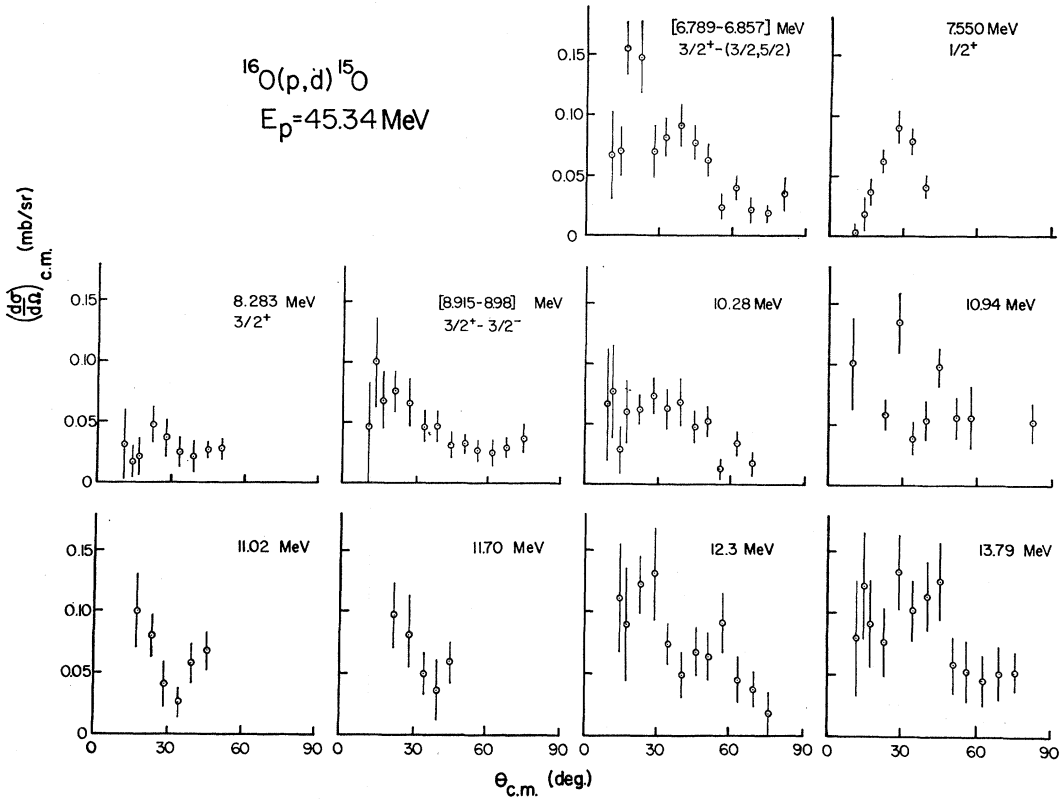

FIG. 10. Deuteron angular distributions for other levels excited in ^{15}O from the $^{16}O(p, d)^{15}O$ reaction at E_p=45.34 MeV.

$\frac{7}{2}^+$ level of ^{15}N. If it were excited by a direct reaction, it would correspond to the pickup of a $1g_{7/2}$ neutron. The angular distribution for this level obtained with 45.34-MeV incident protons is shown in Fig. 9. The calculated $l_n=4$ shape is somewhat similar to the data. An alternative and much more likely process for the excitation of this level is a two-step process in which the 6.13-MeV, 3^- level of ^{16}O is first excited, with the pickup of a $1p$ neutron (probably a $1p_{1/2}$ neutron) following. Evidence for such a process has been found in the $^{12}C(d, {}^3He)^{11}B^*$ (6.67, $\frac{7}{2}^-$) reaction.[49] A $\frac{5}{2}^+$ level could also be excited by the pickup of a $1p_{3/2}$ neutron in a two-step process. The other angular distributions shown in Fig. 10 exhibit little character. However, the 12.30- and 13.79-MeV levels are quite strong (0.12 mb/sr).

V. DWBA ANALYSIS AND SPECTROSCOPIC FACTORS

Several observations about the $^{16}O(p, d)^{15}O$ spectroscopic factors were used in evaluating the results of a DWBA calculation. The simplest shell model predicts spectroscopic factors of 2 and 4 for the 0.0-MeV, $\frac{1}{2}^-$ and the 6.18-MeV, $\frac{3}{2}^-$ levels of ^{15}O, respectively, these being just the numbers of $1p_{1/2}$ and $1p_{3/2}$ neutrons available for pickup. If, however, some of the $1p$ strength lies in other ^{15}O levels of higher excitation, the spectroscopic factors for the 0.0- and 6.18-MeV levels will be reduced, but the sum of the $1p$ spectroscopic factors will still be 6. However, if the ground state of ^{16}O were to contain admixtures of neutrons from other shells, the total number of $1p$ neutrons available for pickup would be less than 6, and since the $1p_{1/2}$ neutrons are less strongly bound than the $1p_{3/2}$ neutrons, one expects the $1p_{1/2}$ subshell to be depleted more than the $1p_{3/2}$ subshell. Thus, one would expect the ratio of the summed $1p_{3/2}$ spectroscopic factors to the summed $1p_{1/2}$ spectroscopic factors to be greater than 2.

Extensive discussions of the DWBA theory may be found in the literature.[1,2,50] The standard calculation employs the local zero-range approximation in which local optical potentials are used and the interaction is assumed to take place at a point. The neglect of finite-range effects has been investigated by Austern *et al.*[51] and proved to be most important in reactions involving large momentum transfers. The inclusion of exact finite range and nonlocality calculations is difficult, but their effects are approximated by the local energy approximation[52,53] as a correction factor which multiplies the

[49] Y. Dupont and M. Chabre, Phys. Letters **26B**, 362 (1968).

[50] W. Tobocman, *Theory of Direct Nuclear Reactions* (Oxford University Press, New York, 1961).

[51] N. Austern, R. M. Drisko, E. C. Halbert, and G. R. Satchler, Phys. Rev. **133**, B3 (1964).

[52] P. J. A. Buttle and L. B. J. Goldfarb, Proc. Phys. Soc. (London) **83**, 701 (1964).

[53] C. M. Perey and F. G. Perey, Phys. Rev. **134**, B353 (1964).

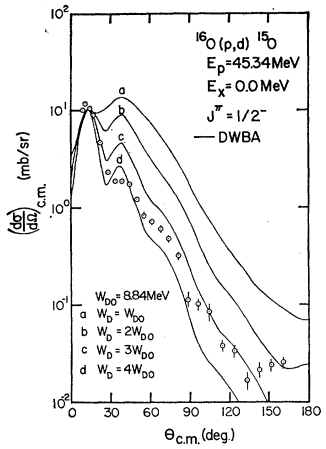

FIG. 11. DWBA fits to the $^{16}O(p, d)^{15}O$, E_p=45.34 MeV, E_x=0.0 MeV, $J^\pi=\frac{1}{2}^-$ angular distribution for different values of the deuteron imaginary-well depth.

zero-range radial form factor, lessening the contribution of the nuclear interior. A FORTRAN version of the Oak Ridge code JULIE[2] was used for all DWBA calculations.

The spectroscopic factor S is extracted from the data by application of the formula

$$S=\sigma_{\text{peak}}/2.25\sigma_{\text{JULIE}}$$

where σ_{peak} is the differential cross section at the characteristic forward peak of the angular distribution, a method successfully used in the past.[3,7] One might expect that the assumption of a direct reaction is more valid for forward angle scattering. It is also thought[54] that exchange terms, which were not included in the transition amplitude, are unimportant at forward angles, but that they might make noticeable contributions at the backward angles. Finally, the fit of the DWBA calculations to the data at forward angles, where most of the integrated cross section is contained, is usually best.

A. 0.0- and 6.18-MeV Levels

Initial DWBA calculations were made for 45.34-MeV incident protons using the optical-model parameters for the entrance and exit channels listed in Tables I and II. The parameters for the bound-state well were r_{0n}= 1.12 F, a_n=0.69 F, and λ=25. The geometric parameters are the same as those of the real proton well, and the value of the spin-orbit strength is the one normally used for nucleons. No lower integration cutoff was used in initial calculations. As can be seen in Fig. 11, the shape of the calculated angular distribution does not match the data. However, in studies of (p, d) reactions in $1p$ shell and $2s$-$1d$ shell nuclei, Kull[3] and Kozub[7] found that an increase in the imaginary-well depth W_D of the deuteron optical potential led to shapes which were in better agreement with the data. Figure 11 shows the results of such calculations in the present case. The shape does improve as W_D increases, but still is not well reproduced. The worst feature, in the present case, is that the magnitude of σ_{peak} decreases from 1.5 to 0.6 mb/sr as W_D increases from W_{D0} to $4W_{D0}$. These values give spectroscopic factors of 3.6 and 8.9, respectively, much too large for $1p_{1/2}$ pickup.

Siemssen *et al.*[55] also encountered the difficulty of reproducing the shape of the data from (d, p) reactions with $1p$ shell nuclei. He obtained reasonable fits by using a lower integration cutoff in the DWBA calculation. Following a similar procedure, W_D was kept at the value found from optical model calculations, and a series of DWBA calculations was made with different values of the lower integration cutoff radius (R_{cut}). The effect of the cutoff radius on σ_{peak} is shown in Fig. 12. Two maxima exist, one at R_{cut}=0 F and one at R_{cut}=3 F. For R_{cut}=0 F one gets a spectroscopic factor for the 0.0-MeV level of 3.2, whereas for R_{cut}=3 F it is 1.8, a much more acceptable value. For the 6.18-MeV level there is no appreciable difference in the spectroscopic factors for R_{cut}=0 F and R_{cut}=3 F. Figures 13 and 14 show the DWBA angular distributions for the ground and 6.18-MeV states. The shape for R_{cut}=3 F is better than for no cutoff but is still not very good. However, the first maximum is reasonably well reproduced, so the prescription of using the measured optical parameters with a lower integration cutoff of 3 F was adopted for all of the DWBA calculations.

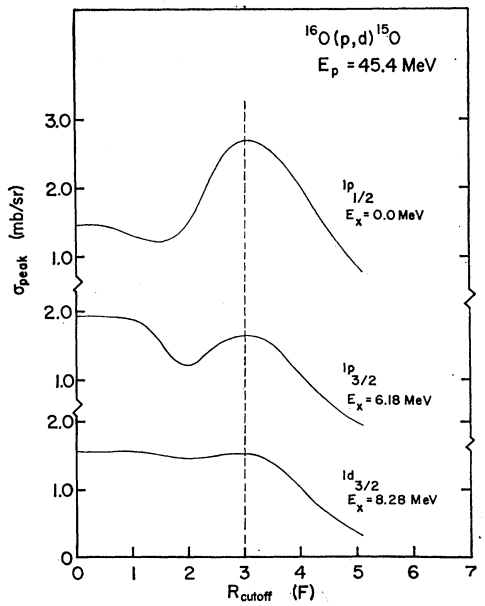

FIG. 12. Dependence of calculated l_n=1 and l_n=2 peak cross sections from the $^{16}O(p, d)^{15}O$ reaction for E_p=35.34 MeV on the value of the lower radial integration cutoff used in the DWBA calculation.

[54] N. Austern, in *Fast Neutron Physics*, edited by J. B. Marion and J. L. Fowler (Wiley-Interscience, Inc., New York, 1963), Vol. II.

[55] R. H. Siemssen, Bull. Am. Phys. Soc. 12, 479 (1967); J. P. Schiffer, G. C. Morrison, R. H. Siemssen, and B. Zeidman, Phys. Rev. 164, 1274 (1967).

Fixing the optical parameters and the integration limits left only the parameters of the bound-state well to be investigated. Since the value of 1.12 F for the radius parameter (r_{0n}) was somewhat smaller than that generally used, calculations were performed for $r_{0n}=1.25$ and 1.35 F. The shapes of the angular distributions were essentially unaltered, but σ_{peak} for the ground state rose from its value of 2.68 mb/sr for $r_{0n}=1.12$ F to 4.35 mb/sr for $r_{0n}=1.35$ F. This represents a lowering of the ground-state spectroscopic factor, the value being 1.51 for $r_{0n}=1.25$ F. This value of the spectroscopic factor is reasonable, but that for the 6.18-MeV, $\frac{3}{2}^-$ level seems much too small since the ratio of the $1p_{3/2}$ to the $1p_{1/2}$ spectroscopic factors is essentially unchanged by the change in r_{0n}. Owing to the lack of significant improvement in the shape and magnitude of the angular distributions with a higher value of r_{0n}, the value of r_{0n} was kept at 1.12 F for the subsequent calculations.

It has been noted that the inclusion of finite-range and nonlocality effects in the DWBA calculations tends to reduce the effect of the nuclear interior. Since this is also the effect of a lower integration cutoff a set of calculations including these effects was made. The code FANLFR2[56] was used to obtain the bound-state form factor which was then used by JULIE in the DWBA calculation. A range of 1.25 F was used with values of the nonlocality parameter β of 0.85 and 0.54 F for protons and deuterons, respectively. The angular distribution shapes were little improved from those calculated using the zero-range approximation with no radial integration cutoff, and a value of 3.0 was obtained for the ground-state spectroscopic factor. If one departs from the accepted value of the range given above and

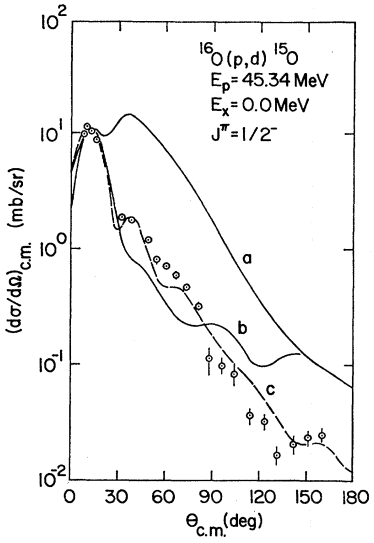

FIG. 13. DWBA fits to the $^{16}O(p, d)^{15}O$, $E_p=45.34$ MeV, $E_x=0.0$ MeV, $J^\pi=\frac{1}{2}^-$ angular distribution for different values of the lower radial integration cutoff of 0.0 for curve a, of 3.0 f for curve b and also using a modified form factor c.

[56] Oak Ridge computer code written by J. K. Dickens.

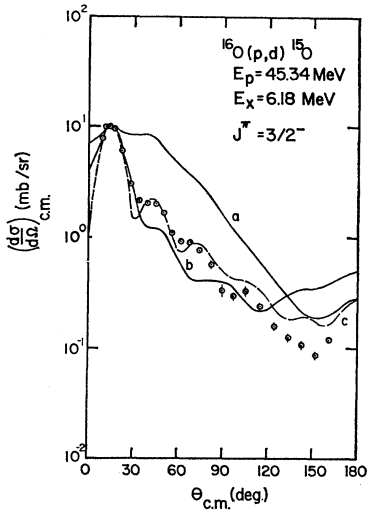

FIG. 14. DWBA fits to the $^{16}O(p, d)^{15}O$, $E_p=45.34$ MeV, $E_x=6.18$ MeV, $J^\pi=\frac{3}{2}^-$ angular distribution for different values of the lower radial integration cutoff of 0.0 for curve a, of 3.0 for curve b and also using a modified form factor c.

increases the value to approximately 2.4 F, the shapes of the calculated angular distributions are greatly improved, but the calculated cross sections are much too small, so these calculations were not used in the present work. Therefore, the use of finite range and nonlocality were abandoned. Recently, it has been pointed out[57] that by application of internal damping to the radial form factor one can get an angular distribution whose shape matches the data well, as shown in Figs. 13 and 14.

Having decided to use a lower integration cutoff with the normal deuteron optical-model parameters, calculations were performed for the 0.0-MeV, $\frac{1}{2}^-$ and 6.18-MeV, $\frac{3}{2}^-$ levels for incident proton energies of 25.52, 31.82, 38.62, and 45.34 MeV. The optical parameters used were those which described elastic scattering at the appropriate energy. The method used in choosing the four proton energies is illustrated in Fig. 15. For an incident proton energy E_p (e.g., 25.52 MeV) the deuterons leaving ^{15}O in the 0.0-MeV, $\frac{1}{2}^-$ state have the same energy in the c.m. frame as those leaving ^{15}O in the 6.18-MeV, $\frac{3}{2}^-$ state when the incident proton energy is E_p' (e.g., 31.82 MeV). Thus, for each pair of energies, reaction data having the same deuteron energies could be compared.

The results of these calculations for 45.34-MeV incident protons are represented by curve b of Figs. 13 and 14. Calculations for the 38.63- and 31.82-MeV protons give similar shapes, but the 25.52-MeV shape is significantly worse. The rather low deuteron energies for this latter case made the assumption of a direct reaction questionable. Spectroscopic factors and ratios of spectroscopic factors for the 0.0- and 6.18-MeV levels are given in Tables III and IV where the errors reflect

[57] B. M. Preedom, J. L. Snelgrove, and E. Kashy (to be published).

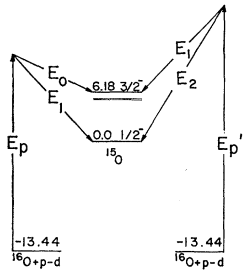

FIG. 15. Basis for the selection of incident proton energies for the $^{16}O(p, d)^{15}O$ experiments.

only the errors in the values of σ_{peak}. The extracted spectroscopic factor for the ground state is constant for the two higher bombarding energies, but it increases for lower values of the incident proton energy. The spectroscopic factor for the 6.18-MeV level rises as the energy of the incident protons decreases from 45 MeV. Table IV shows that the ratios of the spectroscopic factors for these levels is reasonably constant for incident proton energies greater than 30 MeV. The ratios given in the last column are based upon use of the proton energy scheme shown in Fig. 15 to reduce any Q-dependent effects. Only the ratios for the 45.34-MeV data remain unchanged. These data suggest that if reliable spectroscopic factors are to be extracted from the (p, d) reaction on light nuclei, the incident proton energy must be sufficient to produce deuterons having an energy greater than 20 MeV in the c.m. frame. Relative spectroscopic factors appear to be reliable even for lower incident proton energies or, conversely, for higher excitation energies. It is interesting to note here the similarity of the ratio of spectroscopic factors for the 6.18-MeV, $\frac{3}{2}^-$ and 0.0-MeV, $\frac{1}{2}^-$ transitions from the 45.34-MeV data to the ratio of the peak cross sections of these levels from the 100- and 156-MeV data, i.e., 1.3 and 1.6. A DWBA analysis of the 156-MeV $^{16}O(p, d)^{15}O$ data of Bachelier *et al.*[15] by Towner[16] results in spectroscopic factors of 1.70±0.25 and 1.90±0.8 for the 0.0- and 6.18-MeV states, respectively, indicating a serious problem in the form factor used in the analysis. On the other hand, the plane-wave analysis of that same data gave for the ratio of spectroscopic factors a value of 2.0.

TABLE III. Experimental spectroscopic factors for the 0.0- and the 6.18-MeV levels of ^{15}O from the $^{16}O(p, d)^{15}O$ reaction induced by 25.52–45.34-MeV protons.

E_x (MeV)	J^π	E (MeV)	σ_{expt} (mb/sr)	σ_{DWBA} (mb/sr)	S
0.0	$\frac{1}{2}^-$	25.52	6.8±0.5	0.94	3.2±0.2
		31.82	8.5±0.6	1.66	2.3±0.2
		38.63	9.7±0.5	2.38	1.8±0.1
		45.34	11.0±0.8	2.68	1.8±0.1
6.18	$\frac{3}{2}^-$	25.52	2.2±0.2	0.12	8.1±0.7
		31.82	4.5±0.5	0.57	3.4±0.4
		38.63	7.6±0.6	1.14	3.0±0.3
		45.34	10.0±0.7	1.72	2.6±0.2

It is possible to obtain better agreement between the DWBA calculations and the shapes of the experimental angular distributions. Chant *et al.*[11] freely adjusted the deuteron optical-model parameters to obtain the best fit to the ground-state angular distribution from their 30.3 MeV $^{16}O(p, d)^{15}O$ data. The imaginary-well depth was increased by a factor of approximately 3, with changes of 5–20% being made in the other parameters. The fit was very good for the ground-state angular distribution below 78° in the c.m. frame, where the data ended, but the 6.18-MeV fit was not as good. They did not calculate spectroscopic factors, so advisability of such a procedure could not be judged by that criterion. However, the calculations of the present work showed that an increase of the imaginary-well depth led to spectroscopic factors which were much too large.

A study similar to that of the present work has been made by Hiebert *et al.*[10] for proton pickup from ^{16}O. The $^{16}O(d, {}^3He)^{15}N$ reaction was employed with an incident deuteron energy of 34.4 MeV. Satisfactory fits to the data were obtained using standard optical-model potentials. They found that the local finite-range form of the DWBA theory gave the most reliable spectroscopic factors. These values were 2.14 for the 0.0-MeV, $\frac{1}{2}^-$ level of ^{15}N and 3.72 for the 6.33-MeV, $\frac{3}{2}^-$ level. These differ slightly from the present values for neutron pickup from ^{16}O presented in Table III and probably reflect more the uncertainty in the extraction of spectroscopic factors than a dissimilarity of the proton and neutron configurations of the ^{16}O ground state.

TABLE IV. Ratios of experimental spectroscopic factors for the 0.0- and 6.18-MeV levels of ^{15}O from the $^{16}O(p, d)^{15}O$ reaction induced by 25.52–45.34-MeV protons.

E_p^+ (MeV)	E_p^- (MeV)	$\frac{S_{3/2}(E_p^+)}{S_{1/2}(E_p^+)}$	$\frac{S_{3/2}(E_p^+)}{S_{1/2}(E_p^-)}$
25.52	...	2.53±0.25	...
31.82	25.52	1.54±0.15	1.09±0.11
38.63	31.82	1.63±0.16	1.30±0.13
45.34	38.63	1.41±0.14	1.41±0.14

B. Spectroscopic Factors for Other ^{15}O Levels and the Ground State of ^{16}O

Using the criteria established in the previous section, DWBA calculations were performed for other levels in the 45.34-MeV data. The results are similar to those for the strong levels shown in the previous sections. Spectroscopic factors for these levels are given in Table V. Again, the errors quoted reflect only the errors in the experimental value of σ_{peak}. An estimate of the spectroscopic factors for the 5.188- and 5.240-MeV levels was obtained by adding together $2s_{1/2}$ and $1d_{5/2}$ DWBA angular distributions in varying combinations. The results are shown in Fig. 16. A combination of

TABLE V. Peak cross sections and spectroscopic factors for the levels observed in ^{15}O. The average cross section over the indicated angular range is given for weak levels having angular distributions showing no characteristic maximum. The uncertainties quoted in the spectroscopic factors represent only the uncertainties in σ_{peak}.

E_x (MeV)	J^π	l_n	σ_{peak} (mb/sr)	σ_{peak} (deg)	$S(p,d)$
0.0	$\frac{1}{2}^-$	1	11.0±0.8	12 ± 1	1.8±0.1
5.188	$\frac{1}{2}^+$	0			0.02±0.01
5.240	$\frac{5}{2}^+$	2			0.11±0.01
6.180	$\frac{3}{2}^-$	1	10.0±0.7	15 ± 1	2.6±0.2
6.789	$\frac{3}{2}^+$	2	0.08±0.03	20 ± 2	0.02±0.01
6.857	$(\frac{3}{2}, \frac{5}{2})$	2	0.08±0.03	20 ± 2	0.02±0.01
7.284	$(\frac{9}{2}^+, \frac{7}{2}^+)$	(4)	0.12±0.02	45 ± 3	≤0.03±0.01
7.550	$\frac{1}{2}^+$		0.08±0.03	30 ± 3	
8.283	$\frac{3}{2}^+$		0.05±0.02	24 ± 3	0.01±0.005
8.915	$\frac{3}{2}^+$				
8.980	$\frac{3}{2}^-$		0.08±0.04	21 ± 5	0.04±0.02
9.49	$\frac{5}{2}^-$				
9.53	$\frac{1}{2}^+$		0.57±0.05[a]	15 ± 1	
9.60	$\frac{3}{2}^-$	1	0.40±0.07[b]	15 ± 1	0.18±0.03
9.66	$(\frac{7}{2}, \frac{9}{2})^-$				
10.28			0.06±0.02	10− −46	
10.46	$(\frac{3}{2}^-, \frac{1}{2}^-)$	1	0.58±0.06	15 ± 1	0.28±0.03
10.94			0.08±0.03	10− −46	
11.02			0.06±0.02	18− −46	
11.70			0.06±0.02	24− −46	
12.30			0.12±0.05	24 ± 3	
13.79			0.12±0.05	9− −46	

[a] This number represents the combination of the four peaks between 9.49 and 9.66 MeV.

[b] This number represents the estimated contribution of the 9.60-MeV level alone.

$1d_{5/2}$ and $2s_{1/2}$ in the ratio 10 to 1 appears to give the best over-all fit. The spectroscopic factor for the 7.284-MeV, $\frac{7}{2}^+$ level assumes that its excitation is due only to a direct process, thus representing an upper limit.

It is interesting to determine the total $1p$ strength seen in the $^{16}O(p,d)^{15}O$ reaction at 45.34 MeV. By summing the spectroscopic factors for all of the $\frac{1}{2}^-$ and $\frac{3}{2}^-$ levels listed in Table V, we get

$$\sum S(1p_{1/2}) = 1.80, \qquad \sum S(1p_{3/2}) = 3.10,$$

hence

$$\sum S(1p) = 4.90.$$

The relatively low value for the total $1p_{3/2}$ strength indicates the possibility of higher $\frac{3}{2}^-$ levels, as predicted by Bertsch.[44] The $\frac{3}{2}^-$ levels at 9.60 and 10.46 MeV might comprise the $\frac{3}{2}^-$ level predicted by Brown and Shukla[43] to be between 10 and 11 MeV. If it were at 10 MeV, they predict it would have a spectroscopic factor 3% of that of the 6.18-MeV level, whereas the observed value is 18%. An estimate of the $2s$-$1d$ admixtures in the ground state of ^{16}O is contained in the spectroscopic factors for the $\frac{1}{2}^+$, $\frac{5}{2}^+$, and $\frac{3}{2}^+$ levels:

$$\sum S(2s_{1/2}) = \sim 0.02, \qquad \sum S(1d_{5/2}) = 0.15,$$
$$\sum S(1d_{3/2}) = 0.04.$$

The present results can also be compared to those calculated from the ^{16}O ground-state wave function of Brown and Green.[41] This wave function has the form

$$|\,^{16}O_{gs}\rangle = 0.874\,|\,0p\text{-}0h\rangle + 0.469\,|\,2p\text{-}2h\rangle + 0.130\,|\,4p\text{-}4h\rangle,$$

where p is for particles and h is for holes. In the 2p-2h

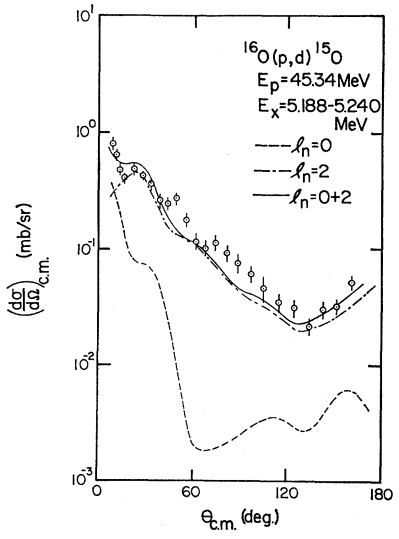

FIG. 16. DWBA fit to the $^{16}O(p,d)^{15}O$, E_p=45.34 MeV, E_x=5.188–5.240 MeV (doublet) angular distribution.

and 4p-4h admixtures one can assume that on the average half of the particles and holes are neutrons, and half protons. Thus, the 0p-0h portion represents six $1p$ neutrons, and the 2p-2h and 4p-4h portions represent five and four $1p$ neutrons, respectively. One would then expect the summed $1p$ spectroscopic factor to be

$$\sum S(1p) = 6(0.874)^2 + 5(0.469)^2 + 4(0.130)^2 = 5.75$$

and

$$\sum S(\text{other}) = 0(0.874)^2 + 1(0.469)^2 + 4(0.130)^2 = 0.25.$$

The sum of the experimental $2s$-$1d$ spectroscopic factors agrees well with this prediction. It appears, then, that as much as 15% of the $1p$ strength could be in levels above 10.46 MeV.

VI. SUMMARY AND CONCLUSIONS

This work has provided valuable information about the use of DWBA calculations in the extraction of spectroscopic factors for the (p, d) reaction on light nuclei. While it is not possible to provide a definite guide for performing meaningful calculations, the effects of variations of certain parameters of the calculation was investigated. The most immediately obvious problem, the inability of a straightforward DWBA calculation to reproduce the shape of the angular distribution, was treated by the use of a lower integration cutoff rather than by changing the deuteron imaginary well depth, which resulted in too large values of the extracted spectroscopic factors. The 3-F cutoff used was a maximum in the σ_{peak}-versus-R_{cut} curve and is close to the value of $1.2A^{1/3}$ for ^{16}O and ^{15}O. In addition to improving the shape of the distribution, the value of the spectroscopic factor became more reasonable.

The radius parameter of the bound-state well (r_{0n}) offers a special problem since the value of the calculated peak cross section, and hence the spectroscopic factor, is a strong function of r_{0n}. One should be aware of this problem in any attempt to extract absolute spectroscopic factors; however, relative spectroscopic factors appear to depend much less strongly on r_{0n}. In the present work a value of r_{0n} equal to the real proton well radius gave reasonable spectroscopic factors.

It also was found that the energy dependence of the peak $l_n=1$ cross sections for the two strongly excited levels of ^{15}O was not reproduced by the DWBA calculation for a deuteron energy in the c.m. frame of less than 20 MeV. Thus, if a (p, d) reaction on a light nucleus is to be performed at a single energy, the proton energy should be as high as practicable. The relative spectroscopic factors showed much less energy dependence than the absolute spectroscopic factors. The use of a method to eliminate some of the Q dependence in the relative spectroscopic factors did not result in any significant improvement and indicates that the problems involved are probably not in the deuteron channel. It may instead be that the high penetrability of the proton is not well accounted for in the DWBA calculation.

The spectroscopic factors extracted from the 45.34-MeV ^{16}O$(p, d)^{15}$O data indicate that about 30% of the $1p_{3/2}$ strength is missing from the 6.18-MeV, $\frac{3}{2}^-$ level. Approximately 12% of this missing strength is contained in the 9.60-MeV, $\frac{3}{2}^-$ and 10.46-MeV, $(\frac{3}{2}^-, \frac{1}{2}^-)$ levels, the latter assignment being made on the basis of the shape of the angular distribution. The 8.98-MeV, $\frac{3}{2}^-$ level contains less than 1% of the $1p_{3/2}$ strength. The remaining strength may reside in many highly fragmented states in the 20-MeV region of excitation.[44] Small $2s$-$1d$ admixtures and a possible $1g_{7/2}$ admixture were observed in the ground state of ^{16}O.

Finally, in view of the various problems in getting spectroscopic factors discussed here one comes to the rather interesting conclusion that the pickup experiment is indeed a better tool for finding out about ground-state admixture in the "unfilled shells" since information as to the occupation number in these shells, even with a 20–40% uncertainty is extremely useful, while the same uncertainty for occupation number of filled or partially filled shells makes such information relatively useless. Conversely, the (d, p) reaction then represents the tool which gives the quantitative measure of hole population for what are normally considered filled orbits.

ACKNOWLEDGMENTS

The authors gratefully acknowledge the assistance of B. M. Preedom and T. Arnette in the use of the optical-model and DWBA codes, and P. J. Plauger, C. Barrows, and B. Horning in acquiring and analyzing the data. We also thank all of the Laboratory staff for their help in building and maintaining the experimental apparatus and in running the cyclotron.